

Accurate calculation of the pressure and temperature of water, steam, and ice: Formulation for CFD[†]

Jang-Chang Lee^{1,*} and Meng-Sing Liou²

¹Department of Mechanical Engineering, Andong National University, Andong, 760-749, Korea

²NASA Glenn Research Center at Lewis Field, Cleveland, Ohio, 44135,

(Manuscript Received February 3, 2010; Revised August 5, 2010; Accepted August 17, 2010)

Abstract

An accurate approach is proposed for calculating the thermodynamic properties of water in three states: liquid, steam and ice, and the transitional states among them. The formulation is expressed in terms of quantities that are naturally used in Computational Fluid Dynamics (CFD), namely the specific volume (v) and specific internal energy (u), through the use of Gibbs free energy. The Gibbs free energy formula proposed by IAPWS, formulated as a function of pressure and temperature, is used as a basis in our calculations. The Jacobian matrix resulting from the transformation between sets of variables (p, T) and (v, u) are derived for each phase; the Newton-Raphson method is used to iteratively solve the nonlinear equations. Numerical calculations have been carried out for the entire phase diagram covering all three phases. The numerical results are compared with the original data of IAPWS and the associated errors are analyzed. It is confirmed that the pressure and temperature are accurately calculated, with largest relative error on the order of 10^{-7} in the ice phase. Hence, other thermodynamic properties are also obtained within the same level of accuracy. The method proposed in this paper for calculating pressure and temperature, variables needed in CFD, is reliable and can be applied to the numerical simulation of multiphase flows, including phase changes.

Keywords: Gibbs free energy; Equation of state for steam; Water, and ice; IAPWS

1. Introduction

Multiphase flows containing water, either as a carrier or dispersed medium are frequently encountered in marine and air vehicles — such as cavitation around hydrofoils, condensation, and icing around airfoils — in which the water may stay in a phase or undergo phase changes depending on the flow and thermodynamic conditions. To achieve an accurate numerical simulation of such flows, it is important to have an accurate description of the thermodynamic property of water, which is supplied as the equation of state (EOS) to the governing equations of the flow. This EOS for water is extremely complex because of the peculiar property of its molecular structure. Of special interest for our purposes is to develop an accurate and efficient procedure for describing steam, water and ice phases.

Many researches of multi-phase flows over the years have used virial equation of state [1-3]. This EOS shows a good agreement with the experimental data of steam, but a substantial deviation from the data of water.

The Van Der Waals EOS unlike virial EOS accounts for the phase change (liquefaction) and is a cubic function including two parameters. These parameters are fitted for a specific substance; they are available in the literature for many common substances. However, this EOS shows that the deviation increases in large densities [4].

The Peng-Robinson EOS is one of many modified Van Der Waals EOS's [4, 5]. The parameter included in this EOS can be found from the experimental data of water-steam ($a = 0.5691$, $b = 0.06864$). This EOS, however, is well matched with steam data but is mismatched with water data. In general, the water density in experimental data decreases parabolically as the temperature increases in the $v - T$ graph, but the water density calculated from the Peng-Robinson EOS decreases linearly. Martin's EOS; is another modified form of the Van Der Waals EOS, it includes three parameters [4]. These parameters, obtained from comparison with the experimental data of water-steam, are $a = 0.3764$, $c = -0.00072$, and $t = -0.00566$. However, this EOS does not agree with experimental data of water as well as the Peng-Robinson EOS.

Clearly, none of available *simple* algebraic EOS models perform satisfactorily in the water phase; the error becomes larger as the water density increases. Hence, we begin by prioritizing

[†]This paper was recommended for publication in revised form by Associate Editor Jun Sang Park

*Corresponding author. Tel.: +82 54 820 5168, Fax: +82 54 820 6127

E-mail address: leejc@andong.ac.kr

© KSME & Springer 2010

accuracy over simplicity, we seek an EOS that can accurately represent all three phases and the transitional states while understanding that it may be mathematically and numerically considerably more complicated than the simple forms just mentioned. The concern for computational cost will only become trivial as computer technologies are advancing in rapid pace. In fact, the calculations presented here took less than a second for steam and water phases and 31 seconds for ice on a Dell PC, CPU 2.66GHz. Thus, we choose to base on the most accurate form of EOS for water developed by IAPWS, and focus on developing a formulation of this EOS to be well-suited for CFD purposes.

2. Gibbs free energy formula

To calculate the thermodynamic properties of water, steam, and ice, IAPWS proposes the formula for each phase using Gibbs free energy [6–8].

The basic equation for the dimensionless specific Gibbs free energy, $\gamma = g/RT$, for water is given as follows:

$$\gamma(\pi, \tau) = \sum_{i=1}^{34} n_i (7.1 - \pi)^{I_i} (\tau - 1.222)^{J_i} \quad (1)$$

where R is the gas constant of water ($R = 0.461526 \text{ [kJ kg}^{-1} \text{ K}^{-1}\text{]}$), π is the pressure ratio, $\pi = p/p^*$, where $p^* = 16.53 \text{ [MPa]}$, and τ is the temperature ratio, $\tau = T^*/T$, with $T^* = 1386 \text{ [K]}$. The coefficients n_i exponents I_i and J_i are given in Table A1 of Appendix. The pressure and temperature ranges for applying the Eq. (1) are as follows (see region 1 of Fig. 1):

$$273.15 \text{ [K]} \leq T \leq 623.15 \text{ [K]}, \quad p_s(T) \leq p \leq 100 \text{ [MPa]},$$

where $p_s(T)$ is a saturated pressure at a given temperature.

The fundamental equation for the dimensionless specific Gibbs free energy, $\gamma = g/RT$, for steam is defined as follows:

$$\gamma(\pi, \tau) = \gamma^0(\pi, \tau) + \gamma^r(\pi, \tau), \quad (2)$$

where γ^0 is ideal gas part and γ^r is residual part; they are defined as follows:

$$\gamma^0 = \ln \pi + \sum_{i=1}^9 n_i^0 \tau^{J_i^0}, \quad (3)$$

$$\gamma^r = \sum_{i=1}^{43} n_i \pi^{I_i} (\tau - 0.5)^{J_i} \quad (4)$$

where $\pi = p/p^*$ and $\tau = T^*/T$ with $p^* = 1 \text{ [MPa]}$ and $T^* = 540 \text{ [K]}$. The coefficients n_i^0 and exponents J_i^0 in Eq. (3) are given in Table A2 of Appendix and the coefficients n_i and exponents I_i and J_i in Eq. (4) are given in Table A3 of Appendix. Eq. (2) covers region 2 of Fig. 1 defined by the

following ranges of temperature and pressure:

$$\begin{aligned} 273.15 \text{ [K]} &\leq T \leq 623.15 \text{ [K]}, \quad 0 \leq p \leq p_s(T) \text{ [MPa]}, \\ 623.15 \text{ [K]} &\leq T \leq 863.15 \text{ [K]}, \quad 0 \leq p \leq p(T) \text{ [MPa]}, \\ 863.15 \text{ [K]} &\leq T \leq 1073.15 \text{ [K]}, \quad 0 \leq p \leq 100 \text{ [MPa]}, \end{aligned}$$

where $p(T)$ is the boundary pressure between region 2 and 3 in Fig. 1 and the equation of $p(T)$ is specified in Ref. [7].

The basic equation for the dimensional specific Gibbs free energy, $g(p, T)$, for ice is defined as follows [8]:

$$\begin{aligned} g(p, T) = g_0 - s_0 T_t \tau \\ + T_t \operatorname{Re} \left\{ \sum_{k=1}^2 r_k \left[(t_k - \tau) \ln(t_k - \tau) \right. \right. \\ \left. \left. + (t_k + \tau) \ln(t_k + \tau) - 2t_k \ln t_k - \frac{\tau^2}{t_k} \right] \right\}. \end{aligned} \quad (5)$$

Here, g_0 and r_2 are defined as follows;

$$\begin{aligned} g_0(p) &= \sum_{k=0}^4 g_{0k} (\pi - \pi_0)^k, \\ r_2(p) &= \sum_{k=0}^2 r_{2k} (\pi - \pi_0)^k. \end{aligned}$$

The dimensionless parameters again are $\pi = p/p_t$ and $\tau = T/T_t$ where $p_t = 611.657 \text{ [Pa]}$ and $T_t = 273.16 \text{ [K]}$ at the triple point. The dimensionless normal pressure is $\pi_0 = p_0/p_t$ where $p_0 = 101325 \text{ [Pa]}$. The coefficients g_{0k} and s_0 in Eq. (5) are real constants, given in Table A4 of Appendix. The complex constants t_1, r_1, t_2 , and $r_{20} \sim r_{22}$ are also given in Table A4. Eq. (5) covers the entire range of ice, where the temperature and pressure ranges are

$$0 \text{ [K]} \leq T \leq 273.16 \text{ [K]}, \quad 0 \text{ [MPa]} \leq p \leq 100 \text{ [MPa]}.$$

All the thermodynamic properties for each phase — specific volume, specific internal energy, specific entropy, specific enthalpy, specific heat capacity, and speed of sound — can be expressed in terms of Gibbs free energy and its derivatives [7].

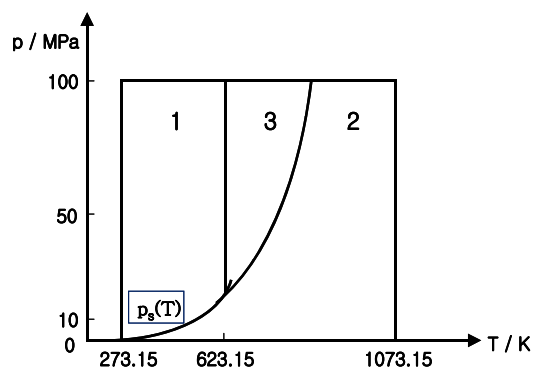


Fig. 1. Regions of IAPWS-IF97.

For example, the specific volume and specific internal energy are defined as follows:

$$v = \left(\frac{\partial g}{\partial p} \right)_T, \quad (6)$$

$$u = g - T \left(\frac{\partial g}{\partial T} \right)_p - p \left(\frac{\partial g}{\partial p} \right)_T. \quad (7)$$

Derivatives in Eq. (6) and Eq. (7) are obtained from Eq. (1), Eq. (2), and Eq. (5). Other thermodynamic properties are also obtained in the same way and the relations of those are specified in Ref. [7]. Other derivatives for all three phases are shown in detail in Ref. [7].

3. Newton-Raphson method

In order to calculate the pressure and temperature of water, steam, and ice from a given specific volume (v) and specific internal energy (u), the Newton-Raphson method is used. The two-equation version of the Newton-Raphson method is formulated as:

$$p_{i+1} = p_i - \frac{(v_i - v_0) \left(\frac{\partial u_i}{\partial T} \right) - (u_i - u_0) \left(\frac{\partial v_i}{\partial T} \right)}{\left(\frac{\partial v_i}{\partial p} \right) \left(\frac{\partial u_i}{\partial T} \right) - \left(\frac{\partial v_i}{\partial T} \right) \left(\frac{\partial u_i}{\partial p} \right)}, \quad (8)$$

$$T_{i+1} = T_i - \frac{(u_i - u_0) \left(\frac{\partial v_i}{\partial p} \right) - (v_i - v_0) \left(\frac{\partial u_i}{\partial p} \right)}{\left(\frac{\partial v_i}{\partial p} \right) \left(\frac{\partial u_i}{\partial T} \right) - \left(\frac{\partial v_i}{\partial T} \right) \left(\frac{\partial u_i}{\partial p} \right)}, \quad (9)$$

where subscript i denotes the known value calculated at the previous iteration and $i+1$ is the unknown value at the present iteration. v_0 and u_0 are given as exact values and v_i and u_i are values calculated using p_i and T_i . As mentioned earlier, all the derivatives in Eq. (8) and Eq. (9) can be derived from the formula of Gibbs free energy for each phase: Eq. (1), Eq. (2), and Eq. (5). The denominator of Eq. (8) and Eq. (9) is called the Jacobian matrix of the system, which results from the transformation between sets of variables (p, T) and (v, u). These nonlinear equations are solved iteratively to get converged solutions of p and T from v_0 and u_0 .

The elements of Jacobian matrix for each phase are derived. Those elements for water from Eq. (1), Eq. (6), and Eq. (7) are

$$\frac{\partial v}{\partial p} = \left(\frac{RT}{p^{*2}} \right) \gamma_{\pi\pi}, \quad (10)$$

$$\frac{\partial v}{\partial T} = \left(\frac{R}{p^*} \right) \gamma_\pi - \left(\frac{R\tau}{p^*} \right) \gamma_{\pi\tau}, \quad (11)$$

$$\frac{\partial u}{\partial p} = \left(\frac{-RT}{p^*} \right) \gamma_\pi + \left(\frac{RT^*}{p^*} \right) \gamma_{\pi\tau} - \left(\frac{RT\pi}{p^*} \right) \gamma_{\pi\pi}, \quad (12)$$

$$\frac{\partial u}{\partial T} = (-R\tau^2) \gamma_{\pi\tau} - (R\pi) \gamma_\pi + (R\pi\tau) \gamma_{\pi\pi}. \quad (13)$$

For steam:

$$\frac{\partial v}{\partial p} = \left(\frac{RT}{p^{*2}} \right) \gamma_{\pi\pi}, \quad (14)$$

$$\frac{\partial v}{\partial T} = \left(\frac{R}{p^*} \right) + \left(\frac{R}{p^*} \right) \gamma_\pi^r - \left(\frac{R\tau}{p^*} \right) \gamma_{\pi\tau}^r, \quad (15)$$

$$\frac{\partial u}{\partial p} = \left(\frac{RT^*}{p^*} \right) \gamma_{\pi\tau}^r - \left(\frac{RT}{p^*} \right) \gamma_\pi^r - \left(\frac{RTp}{p^{*2}} \right) \gamma_{\pi\pi}^r, \quad (16)$$

$$\frac{\partial u}{\partial T} = (-R\tau^2) (\gamma_{\pi\tau}^0 + \gamma_{\pi\tau}^r) - R + \left(\frac{R\pi\tau}{T} \right) \gamma_{\pi\pi}^r. \quad (17)$$

For ice:

$$\begin{aligned} \frac{\partial v}{\partial p} = & g_{0,pp} + T_l \operatorname{Re} \left\{ r_{2,pp} \left[(t_2 - \tau) \ln(t_2 - \tau) \right. \right. \\ & \left. \left. + (t_2 + \tau) \ln(t_2 + \tau) - 2t_2 \ln t_2 - \frac{\tau^2}{t_2} \right] \right\}, \end{aligned} \quad (18)$$

$$\frac{\partial v}{\partial T} = \operatorname{Re} \left\{ r_{2,p} \left[-\ln(t_2 - \tau) + \ln(t_2 + \tau) - \frac{2\tau}{t_2} \right] \right\}, \quad (19)$$

$$\begin{aligned} \frac{\partial u}{\partial p} = & -T \left(\operatorname{Re} \left\{ r_{2,p} \left[-\ln(t_2 - \tau) + \ln(t_2 + \tau) - \frac{2\tau}{t_2} \right] \right\} \right) \\ & - p \left(g_{0,pp} + T_l \operatorname{Re} \left\{ r_{2,pp} \left[(t_2 - \tau) \ln(t_2 - \tau) \right. \right. \right. \\ & \left. \left. \left. + (t_2 + \tau) \ln(t_2 + \tau) - 2t_2 \ln t_2 - \frac{\tau^2}{t_2} \right] \right\} \right), \end{aligned} \quad (20)$$

$$\begin{aligned} \frac{\partial u}{\partial T} = & -T \left(\left(\frac{1}{T_l} \right) \operatorname{Re} \left\{ \sum_{k=1}^2 r_k \left[\frac{1}{(t_k - \tau)} + \frac{1}{(t_k + \tau)} - \frac{2}{t_k} \right] \right\} \right) \\ & - p \left(\operatorname{Re} \left\{ r_{2,p} \left[-\ln(t_2 - \tau) + \ln(t_2 + \tau) - \frac{2\tau}{t_2} \right] \right\} \right). \end{aligned} \quad (21)$$

4. Numerical results

Numerical calculations have been carried out for the thermodynamic properties of each phase and the numerical results are compared with the original data of IAPWS (Tables A5 to A7 of Appendix). The associated errors are analyzed in this paper.

Fig. 2 shows the change of pressure error for water with $T = 300$ [K], $T = 400$ [K], and $T = 500$ [K] for the entire pressure range, $p_s(T) \leq p \leq 100$ [MPa] (see region 1 of Fig. 1). Here, we define $\text{Error}(\%) = (p_0 - p)/p_0 \times 100$ where p_0 is the exact value and p is the calculated value. The verti-

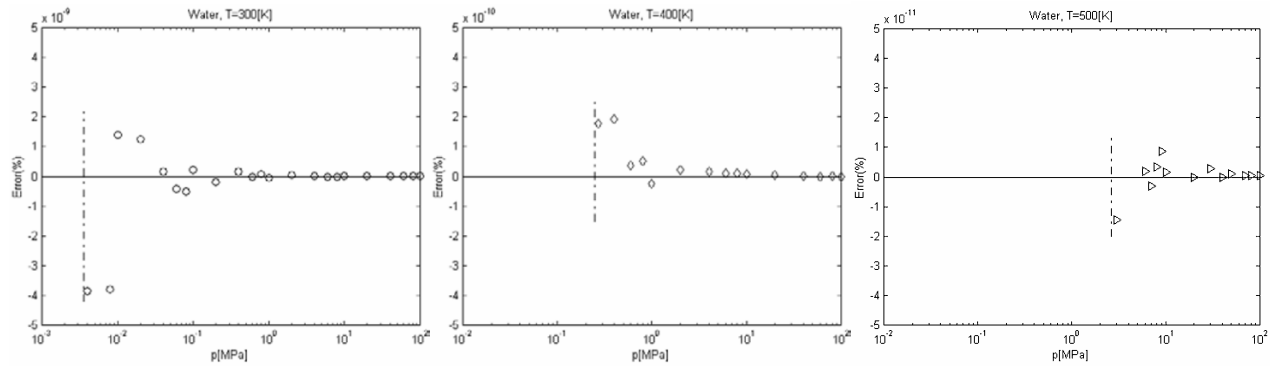


Fig. 2. The change of pressure error for water for the entire pressure range at given temperatures: T=300 [K], T=400 [K], and T=500 [K].

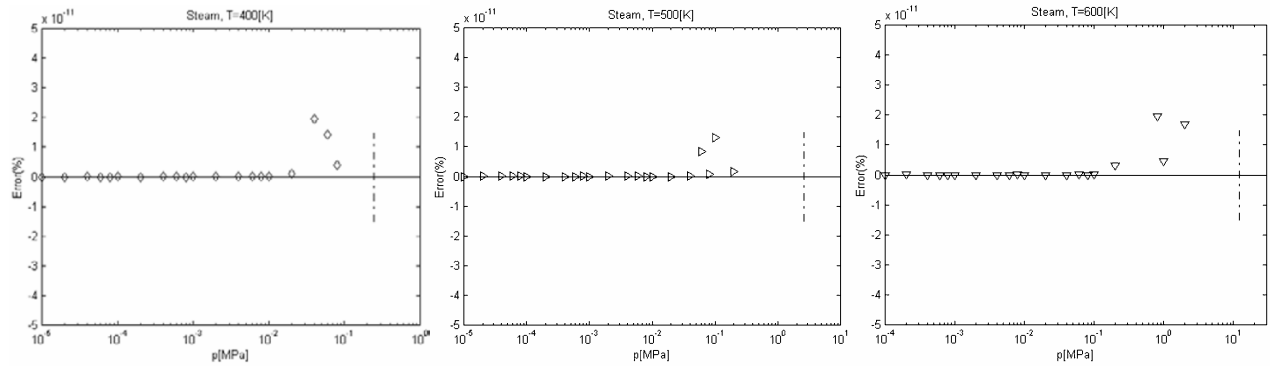


Fig. 3. The change of pressure error for steam for the entire pressure range at given temperatures: T=400 [K], T=500 [K], and T=600 [K].

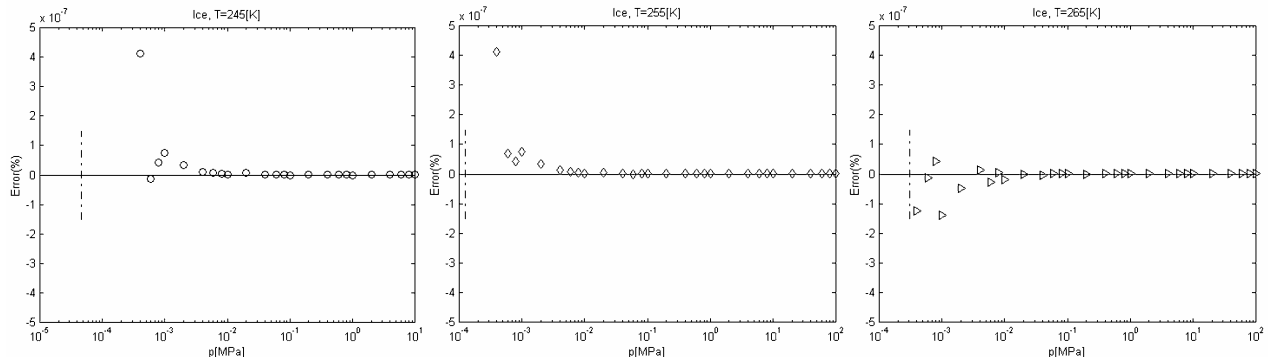


Fig. 4. The change of pressure error for ice for the entire pressure range at given temperatures: T=245 [K], T=255 [K], and T=265 [K].

cal dash-dot line in the graphs represents the saturated pressure at the given temperature. That is, $p_s = 3.53658941 \times 10^{-3}$ [MPa] for $T = 300$ [K], $p_s = 2.47546 \times 10^{-1}$ [MPa] for $T = 400$ [K], and $p_s = 2.63889776 \times 10^0$ [MPa] for $T = 500$ [K]. The deviations are small in the higher pressure region but increase a little in lower pressure region around saturated pressure region. These phenomena are common in all the graphs of Fig. 2. However, since the values of maximum pressure error for given temperatures are extremely small, respectively $O(10^{-9})$, $O(10^{-10})$, and $O(10^{-11})$, the pressure is accurately calculated from a given v and u . In Eq. (8) and Eq. (9), $p = 611.6$ [MPa] and $T = 273.16$ [K] are used as initial

guesses for water.

Fig. 3 represents the change of pressure error for steam with $T = 400$ [K], $T = 500$ [K], and $T = 600$ [K]. In that the steam area corresponds to region 2 of Fig. 1, the pressure range for $273.15[K] \leq T \leq 623.15[K]$ is $0 \leq p \leq p_s(T)$ [MPa]. Hence, the vertical dash-dot lines in the graphs are the saturated pressure and $p_s = 1.23443146 \times 10^1$ [MPa] for $T = 600$ [K]. The pressure errors of steam as well as water are increased near the boundary region, the saturated pressure line, but since the maximum pressure error is $O(10^{-11})$, the calculations of pressure are highly accurate. As initial guess values for Eq. (8) and Eq. (9), $p = 0.001$ [Pa] and $T = 273.16$ [K]

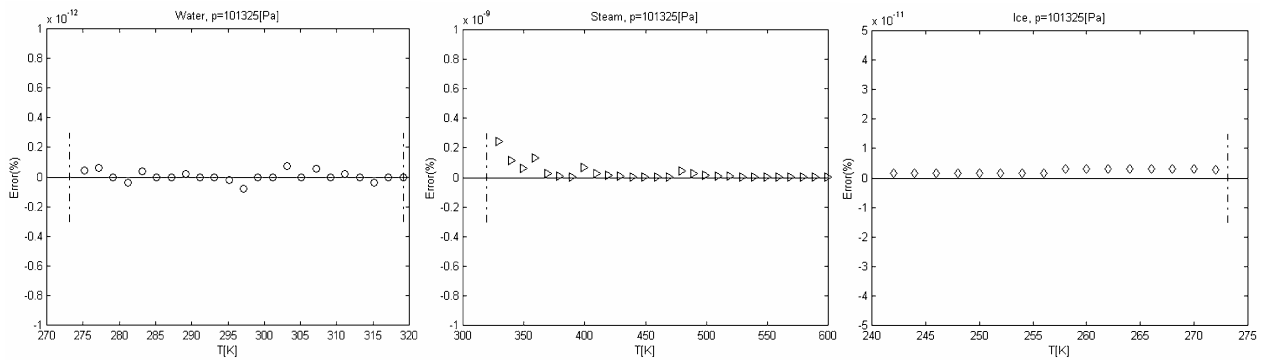


Fig. 5. The change of temperature error for three phases for the entire temperature range at $p = 101325$ [Pa].

for steam are used.

Fig. 4 shows the change of pressure error for ice with $T = 245$ [K], $T = 255$ [K], and $T = 265$ [K]. The pressure and temperature ranges for applying Eq. (5) are $0 \leq p \leq 211$ [MPa] and $0 \leq T \leq 273.16$ [K]. If temperature is below $T = 273.16$ [K], the sublimation pressure line is the boundary between steam and ice (see Fig. 1 the phase-boundary curves of water in a $p-T$ diagram of Ref. [9]). Therefore, the vertical dash-dot line in each graph is the sublimation pressure line at a given temperature and $p_{subl} = 4.601 \times 10^{-5}$ [MPa] for $T = 245$ [K], $p_{subl} = 1.232 \times 10^{-4}$ [MPa] for $T = 255$ [K], and $p_{subl} = 3.059 \times 10^{-4}$ [MPa] for $T = 265$ [K]. In the case of ice, the deviations of pressure error are also increased around the sublimation pressure line but are decreased as the pressure is increased. Since the maximum pressure error is $O(10^{-7})$, the ice pressures are also accurately calculated. Even though the pressure change is large as seen in Table A7 of Appendix, the changes of v and u are very small. To increase convergence of numerical solution, small underrelaxation factors are used to update new iterates if the Jacobian matrices in Eq. (8) and Eq. (9) are small, respectively $O(0.001)$ for P and $O(0.003)$ for T . As initial guess values of Eq. (8) and Eq. (9), $p = 0.0$ [Pa] and $T = 10.0$ [K] for ice are used.

Fig. 5. illustrates the change of temperature error for all three phases with $p = 101325$ [Pa]. Two vertical dash-dot lines in water graph are the melting temperature line, $T = 273.14$ [K], and the saturated temperature line, $T = 319.15$ [K]. The line in the steam graph indicates the saturated temperature, $T = 319.15$ [K] and the line in the ice graph indicates the melting temperature, $T = 273.14$ [K]. Since the maximum temperature error are $O(10^{-12})$, $O(10^{-9})$, and $O(10^{-11})$ respectively, the temperatures are also accurately calculated from given v and u .

5. Conclusions

Using the most extensive and accurate EOS developed by IAPWS by using the Gibbs free energy formula, we develop an accurate procedure to express (p, T) in terms of the set of

variables (v, u) derived directly from the CFD calculations. The thermodynamic properties for all three phases are calculated. The results are compared with the original data of IAPWS. It is confirmed that all the properties are accurately calculated. Numerical results show that the largest relative error among all three phases is $O(10^{-7})$.

The method proposed in this paper for calculating pressure and temperature, variables needed in CFD, is reliable and can be applied to numerical simulation of multiphase flows, including phase changes.

Acknowledgment

This work was supported by a grant from 2007 Research Fund of Andong National University.

Nomenclature

g	: Dimensional specific Gibbs free energy
$g_{00} \sim g_{04}$: Real constants
I_i, J_i	: Exponents of equations
n_i	: Coefficient of equations
P	: Pressure
P_s	: Saturated pressure
R	: Gas constant of water
r_1, r_2, t_1	: Complex constants
$r_{20} \sim r_{22}$: Complex constants
s_0	: Real constants
T	: Temperature
u	: Specific internal energy
u_0	: Exact value of specific internal energy
v	: Specific volume
v_0	: Exact value of specific volume
γ	: Dimensionless specific Gibbs free energy ($\gamma = g / RT$)
γ^0	: Ideal gas part of dimensionless specific Gibbs free energy
γ^r	: Residual part of dimensionless specific Gibbs free energy
π	: Pressure ratio ($\pi = p / p^*$)

τ : Temperature ratio ($\tau = T^* / T$)

Subscripts

$subl$: Sublimation
 t : Triple point

References

- [1] P. P. Wegener and L. M. Mack, Condensation in Supersonic and Hypersonic Wind Tunnels, *Advances in Applied Mechanics*, edited by Dryden/Karman, Academic, 5 (1958) 307-447.
- [2] G. H. Schnerr and U. Dohrmann, Transonic Flow around Airfoils with Relaxation and Energy Supply by Homogeneous Condensation, *AIAA J.* 28 (1990) 1187-1193.
- [3] A. Berg, U. Iben, A. Meister and J. Schmidt, Modeling and Simulation of Cavitation in Hydraulic Pipelines Based on the Thermodynamic and Caloric Properties of Liquid and Steam, *Shock Waves*, 14 (2005) 111-121.
- [4] J. W. Tester and M. Modell, Thermodynamics and its Applications, third Ed. Prentice Hall International Series in the Physical Chemical Engineering Sciences (1996).
- [5] Z. Xu and S. I. Sandler, Temperature -Dependent Parameters and the Peng-Robinson Equation of State, *Ind. Eng. Chem. Res.*, 26 (3) (1987) 601-606.
- [6] W. Wagner, et. al, The IAPWS Industrial Formulation 1997 for the Thermodynamic Properties of Water and Steam, *J. of Engineering for Gas Turbines and Power*, 122 (2000) 150-182.
- [7] Erlangen, The International Association for the Properties of Water and Steam, (Release on the IAPWS Industrial Formulation 1997 for the Thermodynamic Properties of Water and Steam), Germany, (1997) 1- 48.
- [8] R. Feistel and W. Wagner, A New Equation of State for H₂O Ice Ih, *J. Phys. Chem. Ref. Data*, 35 (2) (2006) 1021-1047.
- [9] W. Wagner, A. Saul and A. Pruss, International Equations for the Pressure along the Melting and along the Sublimation Curve of Ordinary Water Substance, *J. Phys. Chem. Ref. Data*, 23 (3) (1994) 515-527.
- [10] W. Wagner and A. Pruss, International Equation for the Saturation Properties of Ordinary Water Substance. Revised According to the International Temperature Scale of 1990, *J. Phys. Chem. Ref. Data*, 22 (3) (1993) 783-787.
- [11] S. C. Chapra and R. P. Canale, Numerical Methods for engineers, Fifth Ed. McGraw-Hill, New York, USA (2007).

Appendix

Table A1. Coefficients and exponents of Eq. (1).

i	I_i	J_i	n_i
1	0	-2	0.14632971213167
2	0	-1	-0.84548187169114
3	0	0	-0.37563603672040 × 10 ¹
4	0	1	0.33855169168385 × 10 ¹
5	0	2	-0.95791963387872

6	0	3	0.15772038513228
7	0	4	-0.1661641799501 × 10 ⁻¹
8	0	5	0.81214629983568 × 10 ⁻³
9	1	-9	0.28319080123804 × 10 ⁻³
10	1	-7	-0.60706301565874 × 10 ⁻³
11	1	-1	-0.18990068218419 × 10 ⁻¹
12	1	0	-0.32529748770505 × 10 ⁻¹
13	1	1	-0.21841717175414 × 10 ⁻¹
14	1	3	-0.52838357969930 × 10 ⁻⁴
15	2	-3	-0.47184321073267 × 10 ⁻³
16	2	0	-0.30001780793026 × 10 ⁻³
17	2	1	0.47661393906987 × 10 ⁻⁴
18	2	3	-0.44141845330846 × 10 ⁻⁵
19	2	17	-0.72694996297594 × 10 ⁻¹⁵
20	3	-4	-0.31679644845054 × 10 ⁻⁴
21	3	0	-0.28270797985312 × 10 ⁻⁵
22	3	6	-0.85205128120103 × 10 ⁻⁹
23	4	-5	-0.22425281908000 × 10 ⁻⁵
24	4	-2	-0.65171222895601 × 10 ⁻⁶
25	4	10	-0.14341729937924 × 10 ⁻¹²
26	5	-8	-0.40516996860117 × 10 ⁻⁶
27	8	-11	-0.12734301741641 × 10 ⁻⁸
28	8	-6	-0.17424871230634 × 10 ⁻⁹
29	21	-29	-0.68762131295531 × 10 ⁻¹⁸
30	23	-31	-0.14478307828521 × 10 ⁻¹⁹
31	29	-38	0.26335781662795 × 10 ⁻²²
32	30	-39	-0.11947622640071 × 10 ⁻²²
33	31	-40	0.18228094581404 × 10 ⁻²³
34	32	-41	-0.93537087292458 × 10 ⁻²⁵

Table A2. Coefficients and exponents of Eq. (3).

i	J_i^0	n_i^0
1	0	-0.96927686500217 × 10 ¹
2	1	-0.10086655968018 × 10 ²
3	-5	-0.56087911283020 × 10 ⁻²
4	-4	0.71452738081455 × 10 ⁻¹
5	-3	-0.40710498223928
6	-2	-0.14240819171444 × 10 ¹
7	-1	-0.43839511319450 × 10 ¹
8	2	-0.28408632460772
9	3	0.21268463753307 × 10 ⁻¹

Table A3. Coefficients and exponents of Eq. (4).

i	I_i	J_i	n_i
1	1	0	-0.17731742473213 × 10 ⁻²
2	1	1	-0.17834862292358 × 10 ⁻¹
3	1	2	-0.45996013696365 × 10 ⁻¹
4	1	3	-0.57581259083432 × 10 ⁻¹
5	1	6	-0.50325278727930 × 10 ⁻¹
6	2	1	-0.33032641670203 × 10 ⁻⁴
7	2	2	-0.18948987516315 × 10 ⁻³
8	2	4	-0.39392777243355 × 10 ⁻²
9	2	7	-0.43797295650573 × 10 ⁻¹
10	2	36	-0.26674547914087 × 10 ⁻⁴
11	3	0	0.20481737692309 × 10 ⁻⁷
12	3	1	0.43870667284435 × 10 ⁻⁶
13	3	3	-0.32277677238570 × 10 ⁻⁴
14	3	6	-0.15033924542148 × 10 ⁻²
15	3	35	-0.40668253562649 × 10 ⁻¹
16	4	1	-0.78847309559367 × 10 ⁻⁹
17	4	2	0.12790717852285 × 10 ⁻⁷
18	4	3	0.48225372718507 × 10 ⁻⁶
19	5	7	0.22922076337661 × 10 ⁻⁵

20	6	3	$-0.16714766451061 \times 10^{-10}$
21	6	16	$-0.2117147231355 \times 10^{-2}$
22	6	35	$-0.23895741934104 \times 10^2$
23	7	0	$-0.59059564324270 \times 10^{-17}$
24	7	11	$-0.12621808899101 \times 10^{-5}$
25	7	25	$-0.38946842435739 \times 10^{-1}$
26	8	8	$0.11256211360459 \times 10^{-10}$
27	8	36	$-0.82311340897998 \times 10^1$
28	9	13	$0.19809712802088 \times 10^{-7}$
29	10	4	$0.10406965210174 \times 10^{-18}$
30	10	10	$-0.10234747095929 \times 10^{-12}$
31	10	14	$-0.10018179379511 \times 10^{-8}$
32	16	29	$-0.80882908646985 \times 10^{-10}$
33	16	50	0.10693031879409
34	18	57	-0.33662250574171
35	20	20	$0.89185845355421 \times 10^{-24}$
36	20	35	$0.30629316876232 \times 10^{-12}$
37	20	48	$-0.42002467698208 \times 10^{-5}$
38	21	21	$-0.59056029685639 \times 10^{-25}$
39	22	53	$0.37826947613457 \times 10^5$
40	23	39	$-0.12768608934681 \times 10^{-14}$
41	24	26	$0.73087610595061 \times 10^{-28}$
42	24	40	$0.55414715350778 \times 10^{-16}$
43	24	58	$-0.94369707241210 \times 10^{-6}$

Table A4. Coefficients of Eq. (5).

Coefficient	Real constant	Unit
g_{00}	-632020.233449497	J kg^{-1}
g_{01}	0.655022213658955	J kg^{-1}
g_{02}	$-1.89369929326131 \times 10^{-8}$	J kg^{-1}
g_{03}	$3.39746123271053 \times 10^{-15}$	J kg^{-1}
g_{04}	$-5.56464869058991 \times 10^{-22}$	J kg^{-1}
s_0	-3327.33756492168	$\text{J kg}^{-1}\text{K}^{-1}$
Coefficient	Complex constant (real part)	Unit
t_1	$3.68017112855051 \times 10^{-2}$	
r_1	44.7050716285388	$\text{J kg}^{-1}\text{K}^{-1}$
t_2	0.337315741065416	
r_{20}	-72.597457432922	$\text{J kg}^{-1}\text{K}^{-1}$
r_{21}	$-5.57107698030123 \times 10^{-5}$	$\text{J kg}^{-1}\text{K}^{-1}$
r_{22}	$2.34801409215913 \times 10^{-11}$	$\text{J kg}^{-1}\text{K}^{-1}$
Coefficient	Complex constant (real part)	Unit
t_1	$5.10878114959572 \times 10^{-2}$	
r_1	65.6876847463481	$\text{J kg}^{-1}\text{K}^{-1}$
t_2	0.335449415919309	
r_{20}	-78.100842711287	$\text{J kg}^{-1}\text{K}^{-1}$
r_{21}	$4.64578634580806 \times 10^{-5}$	$\text{J kg}^{-1}\text{K}^{-1}$
r_{22}	$-2.85651142904972 \times 10^{-11}$	$\text{J kg}^{-1}\text{K}^{-1}$

Table A5. Thermodynamics properties for water.

Property	$T=300 [\text{K}], p=3 [\text{MPa}]$
$v/(\text{m}^3\text{kg}^{-1})$	$0.100215168 \times 10^{-2}$
$u/(\text{kJ kg}^{-1})$	0.112324818×10^3
$h/(\text{kJ kg}^{-1})$	0.115331273×10^3
$s/(\text{kJ kg}^{-1}\text{K}^{-1})$	0.392294792
Property	$T=300 [\text{K}], p=80 [\text{MPa}]$
$v/(\text{m}^3\text{kg}^{-1})$	$0.971180894 \times 10^{-3}$
$u/(\text{kJ kg}^{-1})$	0.106448356×10^3
$h/(\text{kJ kg}^{-1})$	0.184142828×10^3
$s/(\text{kJ kg}^{-1}\text{K}^{-1})$	0.368563852
Property	$T=500 [\text{K}], p=3 [\text{MPa}]$
$v/(\text{m}^3\text{kg}^{-1})$	$0.120241800 \times 10^{-2}$
$u/(\text{kJ kg}^{-1})$	0.971934985×10^3
$h/(\text{kJ kg}^{-1})$	0.975542239×10^3
$s/(\text{kJ kg}^{-1}\text{K}^{-1})$	0.258041912 $\times 10^1$

Table A6. Thermodynamics properties for ice.

Property	$T=273.16 [\text{K}], p=611.657 [\text{Pa}]$
$v/(\text{m}^3\text{kg}^{-1})$	$1.0908581273664 \times 10^{-3}$
$u/(\text{J kg}^{-1})$	-333444.921310135
$h/(\text{J kg}^{-1})$	-333444.254079125
$s/(\text{J kg}^{-1}\text{K}^{-1})$	-1220.69433939687
Property	$T=273.152519 [\text{K}], p=101325 [\text{Pa}]$
$v/(\text{m}^3\text{kg}^{-1})$	$1.09084388214311 \times 10^{-3}$
$u/(\text{J kg}^{-1})$	-333465.403506706
$h/(\text{J kg}^{-1})$	-333354.873750348
$s/(\text{J kg}^{-1}\text{K}^{-1})$	-1220.76932549696

Table A7. Thermodynamics properties for steam.

Property	$T=300 [\text{K}], p=0.0035 [\text{MPa}]$
$v/(\text{m}^3\text{kg}^{-1})$	0.394913866×10^2
$u/(\text{kJ kg}^{-1})$	0.241169160×10^4
$h/(\text{kJ kg}^{-1})$	0.254991145×10^4
$s/(\text{kJ kg}^{-1}\text{K}^{-1})$	0.852238967 $\times 10^1$
Property	$T=700 [\text{K}], p=0.0035 [\text{MPa}]$
$v/(\text{m}^3\text{kg}^{-1})$	0.923015898×10^2
$u/(\text{kJ kg}^{-1})$	0.301262819×10^4
$h/(\text{kJ kg}^{-1})$	0.333568375×10^4
$s/(\text{kJ kg}^{-1}\text{K}^{-1})$	0.101749996 $\times 10^2$
Property	$T=700 [\text{K}], p=30 [\text{MPa}]$
$v/(\text{m}^3\text{kg}^{-1})$	0.542946619×10^2
$u/(\text{kJ kg}^{-1})$	0.246861076×10^4
$h/(\text{kJ kg}^{-1})$	0.263149474×10^4
$s/(\text{kJ kg}^{-1}\text{K}^{-1})$	0.517540298 $\times 10^1$



Meng-Sing Liou is a Senior Technologist of GRC, for Airbreathing Propulsion Computational Analysis. He has more than 30 years experiences in Computational Fluid Dynamics, contributing in the development of numerical methods and supporting NASA's aeronautics programs since joining NASA in 1986. His AUSM schemes have been adopted in major commercial and research codes, and included in textbooks and CFD courses worldwide. Currently he is leading the Multidisciplinary Design Analysis and Optimization research in the Aeropropulsion Division to support Fundamental Aeronautics Program. He was Chief of Computational Fluid Dynamics. He was awarded NASA's Exceptional Scientific Achievement Medal (1992) and Exceptional Achievement Medal (2004), and the Abe Silverstein Medal (2006). He has published over 200 technical papers, and 8 book chapters. He also gave numerous short courses in various countries. He is an Adjunct Professor of University of California, Santa Barbara and Case Western Reserve University.



Jang-Chang Lee received his B.S. and M.S. degrees in Mechanical Engineering from Chung-Ang University, Korea, in 1989 and 1991, respectively. He then received his Ph.D. degrees from R.P.I. in 2000. Dr. Lee is currently a Professor at Department of Mechanical Engineering at Andong National University in Andong, Korea. Dr. Lee's research interests include Two-phase flows, Aerodynamics.